CHAPTER-1

Introduction

In this chapter, we have highlighted the objectives of the thesis by examining the progress in this field. We have explored the principles of electrochemical water oxidation, its importance in energy conversion and storage, and the parameters used for its evaluation. Additionally, we reviewed previously reported MOF-derived LDHs for OER, noting various shortcomings in this area. Furthermore, we discussed the benefits of using ZIF-67 as a precursor for synthesizing OER catalysts.

1. Introduction

Currently, the fast depletion of fossil fuels and the deterioration of the environment due to global warming caused by carbon dioxide emissions largely stimulate the development of clean sources of energy.[1][2] In this context, hydrogen gas has emerged as a potential source of clean energy owing to its negligible carbon content, harmless end by-product, and highest gravimetric energy density.[3] Thus, hydrogen being the most promising and cleanest energy carrier has replaced the conventional sources of energy. [4] The three main processes used to produce H_2, nowadays are steam methane reforming, coal gasification, and biomass conversion. These processes are not only costly, but they also release a large quantity of CO_2, which will unavoidably have an impact on the greenhouse effects.[5] [6] To overcome this situation, photocatalytic and electricity-driven water splitting have emerged as the most promising and practical approaches for the massive production of hydrogen gas with high purity viable approach for renewable energy conversion.[7] [8] Out of them electrochemical water splitting is regarded as one of the simplest and cheapest methods for the production of hydrogen gas.[9] Electrochemical water splitting is performed in an electrolyzer containing an anode for water oxidation and a cathode for water reduction reactions with a suitable electrolyte for transporting charges and ions between electrodes.[10]

The complete procedure of electrochemical water splitting (EWS) involves two distinct half-cell reactions: the hydrogen evolution reaction (HER) and the oxygen evolution reaction (OER) taking place at the cathode and at the anode respectively.[11][12] When a potential greater than 1.23 V is applied, water reduction and water oxidation occur leading to the generation of hydrogen and oxygen gases which are released from the electrode surfaces.[13]

In our thesis, we have dealt with OER as it plays very crucial role in the various energy storage and conversion devices such as water electrolyzers and metal-air batteries. The OER is responsible

for supplying the protons and electrons, required to transform renewable electricity into chemical fuels.[14] Therefore, development of efficacious and enduring electrocatalysts for the OER has been a major focus of research in applied electrochemistry.

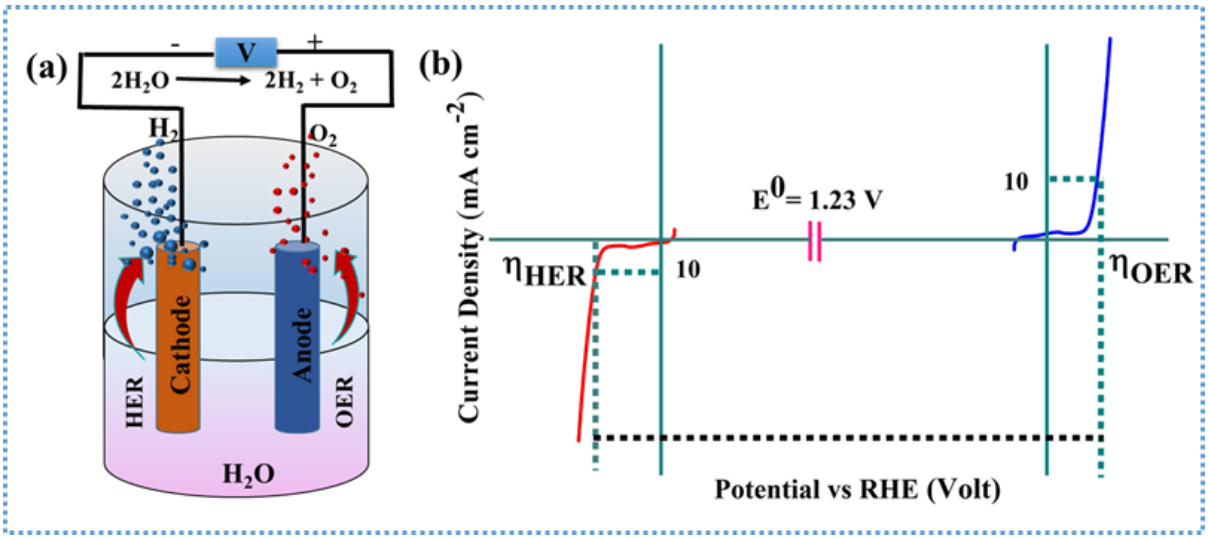

Figure 1.1. (a) Schematic representation for the electrochemical water splitting process, depicting the anodic OER and cathodic HER; (b) Graph displaying the relationship between potential and current density for OER and HER.

1.1. Electrochemical Water Oxidation

As mentioned above, OER is a crucial half-cell process in electrochemical water splitting which occurs at the anode. OER produces molecular oxygen gas through the electrochemical oxidation of water.[15] It has garnered a lot of interest from material scientists in the past 10 years due to its significant role in energy storage/conversion systems like fuel cells, carbon dioxide (CO_2) reduction, rechargeable metal-air batteries, and water splitting.[16] But OER is a complex process and the rate of reaction is very slow as it follows four-step electron transfer mechanism. Therefore, to overcome this issue, the OER requires affordable, efficient, and stable electrocatalysts. [17] [18]

1.2. Electrocatalytic kinetic parameters for OER

The primary assessment criteria for the evaluation of the OER activity of an electrocatalyst

includes some fundamental parameters like overpotential at a specified current density, electrochemical surface area (ECSA), Tafel slope, , turnover frequency (TOF), and faradaic efficiency. [19] All these have been specified below

1.2.1. Overpotential (η)

The use of overpotential becomes crucial in order to surmount the kinetic barriers caused by the raised activation energies necessary for the production of reaction intermediates. It is generally found that the standard free energy change (ΔG) for electrochemical OER's is 4.92 eV. In case of an ideal OER, every elementary stage of producing *OH, *O, *OOH, and O_2, requires free energy (ΔG) of 1.23 eV (4.92 eV/4 ¼ 1.23 eV).[20] If any of these intermediates is strongly coupled to the active metal site, then a larger ΔG is needed for the electron transfer process. Consequently, in order to move forward the entire OER process, an additional potential also referred as an overpotential, is needed.[21] Thus, overpotential refers to the extra voltage required to initiate a reaction beyond its theoretical thermodynamic threshold and plays a crucial role in electrochemical systems and can be calculated by applying the following formula-

$$\eta OER = E_{RHE} - 1.23 \quad (1)$$

It is worth mentioning here that the catalyst with a low overpotential is considered the most active

1.2.2. Tafel slope

Conducting Tafel analysis on the OER process offers insights into the intrinsic kinetics of the electrocatalyst. The Tafel slope typically pertains to the electrochemical reaction mechanism.

The formula for the Tafel slope is determined from Butler-Volmer equation, which provides a logarithmic relationship between overpotential (η) and current density (j) as follows:

$$d \log j/d\eta = (2.303RT/\alpha nF) \quad (2)$$

Where, R stands for gas constant, T stands for temperature, α denotes charge transfer coefficient,

n denotes the number of electron- transferred, F represents the Faraday constant. And the quantity d log j/dη is known as Tafel slope. From the equation (2) it is clear that Tafel slope is inversely proportional to the charge transfer coefficient hence the catalysts with smaller Tafel slope are considered as better catalysts.

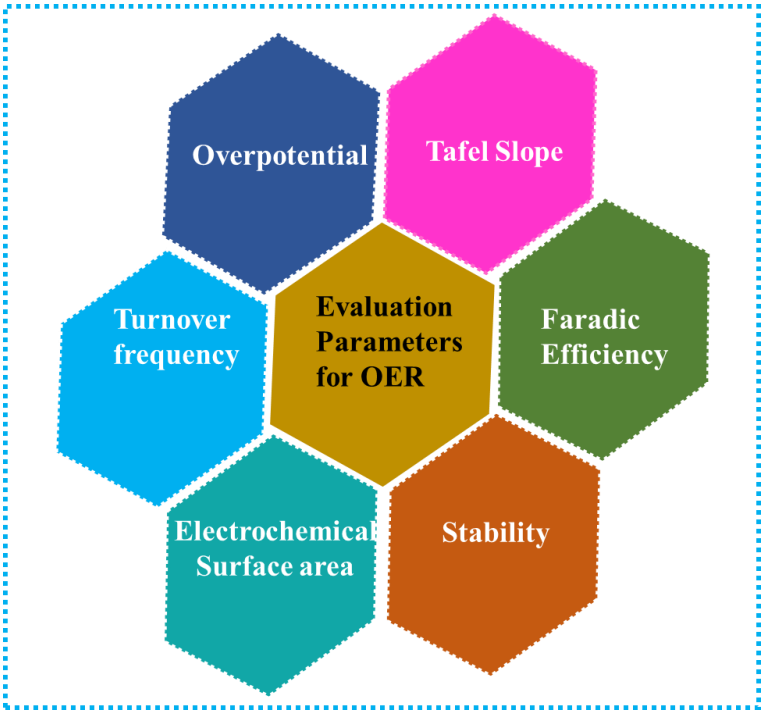

Figure 1.2. Displays the different types of OER kinetic parameters.

From the above equation it is clear that the Tafel slope has an inverse relationship with the charge transfer coefficient (α) and electron count (n). Lower Tafel slopes suggest better electrocatalytic kinetics since they allow the current density to rise more quickly with less overpotential shift (Figure.1.3 b). [22]

1.2.3. Faradaic Efficiency

Faradaic efficiency (FE) is another additional criterion for the evaluation of activity that shows how efficiently the electrons participate in the reaction. FE for OER is defined as the ratio of the

quantity of produced oxygen to the theoretically obtained quantity. Generally, the amount of oxygen is evaluated through the chronoamperometric or chronopotentiometry analysis. Conventional water-gas displacement method, Gas chromatography, and fluorescence spectroscopy are used to detect the practically obtained oxygen.[23] Generally FE for OER process can be calculated using rotating ring disc electrode (RRDE) by applying the following formula:

$$FE = \frac{I_R\, n_D}{I_D\, n_R\, N_{CL}} \qquad (3)$$

Where I_R and I_D are representing the ring current and disc current (mA) respectively. n_R and n_D represent the number of electrons exchanged at the ring and disk, respectively and N_{CL} represents the collection efficiency of the RRDE and N_{CL} has no unit as it is given by the ratio of ring current ($I_{R)}$ and disc current (I_D).

1.2.4 Turnover Frequency (TOF)

Turnover frequency (TOF) is another kinetic parameter that gives the information about the intrinsic activity of an electrocatalyst at a definite overpotential, whose value can be evaluated by the well-known formula as follows-

$$TOF = \frac{jNA}{nF\Gamma} \qquad (4)$$

Where N_A represents the Avogadro constant, Γ is the surface or the total concentration of active sites or the number of atoms taking part in the rection, j refers to the current density, n denotes the number of transferred electrons, and F is the Faraday constant.

From equation (4) it can be concluded that the greater the TOF, the better the catalytic activity of the catalyst will be. Since, both HER and OER follow the pseudo-first-order kinetics and therefore, both have TOF value in terms of time. The mass loading, shape, size, and morphology of the catalyst have no impact on the TOF of an electrocatalyst.[24] The TOF has been utilized in several recent research, however many of them are computed improperly. The key challenge in estimating

TOF for an electrocatalyst is the need for precise information on the exact number of active sites, the real or electrochemical surface area, and the FE, all of which are difficult to obtain. The real or electrochemical surface area and FE are relatively easy to calculate, but determining the number of active sites involved in the reaction is more challenging.[25]

1.2.5. Stability

Stability is a key factor that can be used to determine whether catalysts can be employed in commercial and industrial applications of electrochemical water splitting. Excellent stability is crucial in order to access the practical application. Transition metal compounds, usually demonstrate excellent stability in alkaline electrolytes. However, the majority of them are unable to function correctly because of degradation and dissolving in acidic solutions, and they exhibit OER activity deterioration with the drop in pH, which is dreadfully anticipated from a commercial aspect. There has been a growing emphasis on improving catalyst stability, and it has been shown that modulating the structure of the working electrode is a crucial factor in achieving this goal. In general, catalysts that are grown directly on the working electrode (referred to as self-supporting electrodes) exhibit greater stability compared to those that are drop-casted.

Furthermore, the stability can be assessed through constant polarization at a fixed potential (using chronoamperometry, represented as I-t curve) or at a constant current density (using chronopotentiometry, represented as U-t curve) for a duration of several hours or longer. A catalyst is considered stable for OER when it maintains a consistent current density during chronoamperometry or shows only a minimal rise in overpotential during chronopotentiometry.

Furthermore, a range of methods can be applied to assess the stability in terms of morphology, structure, and composition. These include ex-situ and in-situ techniques such as scanning electron microscopy (SEM), transmission electron microscopy (TEM), X-ray photoelectron spectroscopy

(XPS), inductively coupled plasma analysis, and X-ray diffraction analysis. All the mentioned characterization techniques can be in-situ as well as ex-situ. In our case, we did all characterization in ex-situ manner.

1.2.6. Electrochemical active surface

The most important features of heterogeneous catalysts are high surface area and porosity as these characteristics not only provide exposure of the catalytically active sites but also enable easier diffusion of reactive molecules.[26] The initial step in calculating the electrochemical surface area (ECSA) often involves the determination of the double-layer capacitance (C_{dl}) of the material. This is achieved by constructing cyclic voltammetry (CV) curves at various scan rates within a small potential range, preferably maintaining scan speeds below 100 mV s^{-1}. In this reference, the charging currents at different scan rates, are measured for both anodic and cathodic regions.When the graph is plotted between the scan rate and the difference in double-layer charging current densities (Δj(ja -jc)), the obtained plot exhibits a linear relationship, where the slope corresponds to the double-layer capacitance (C_{dl}) Figure.1.3 d).[27] The following formula can be used to evaluate the electrochemical Surface Area (ECSA) of the sample -

$$\text{ECSA} = \frac{C_{dl}}{C_s} \quad (5)$$

In the above equation, C_s represents either the specific capacitance of the sample or the capacitance of a perfectly smooth planar surface of the material, measured under the same experimental conditions. Following formula was derived from ECSA to the roughness factor of a materials.

$$\text{RF} = \frac{ECSA}{SA_{geo}} \quad (6)$$

Where, SA_{geo} stands for geometrical surface area.

It is worth here to mention that the catalysts with large ECSA are considered because large ECSA

provides more active sites for redox reactions, thereby increasing the rate of electrochemical processes.

1.2.7. Electrochemical impedance spectroscopy (EIS)

Electrochemical impedance spectroscopy (EIS) is a robust method for studying and comprehending the kinetics of interface reactions between electrolytes and electrocatalysts.[28] Impedance (Z) is closely related to resistance; it measures how much a circuit opposes the flow of current. While resistance specifically applies to ideal resistors, real-world circuits are often more complex and do not strictly obey Ohm's law-particularly across different frequencies or when there is a phase shift between voltage and current. In such cases, impedance is used instead of simple resistance.[29]

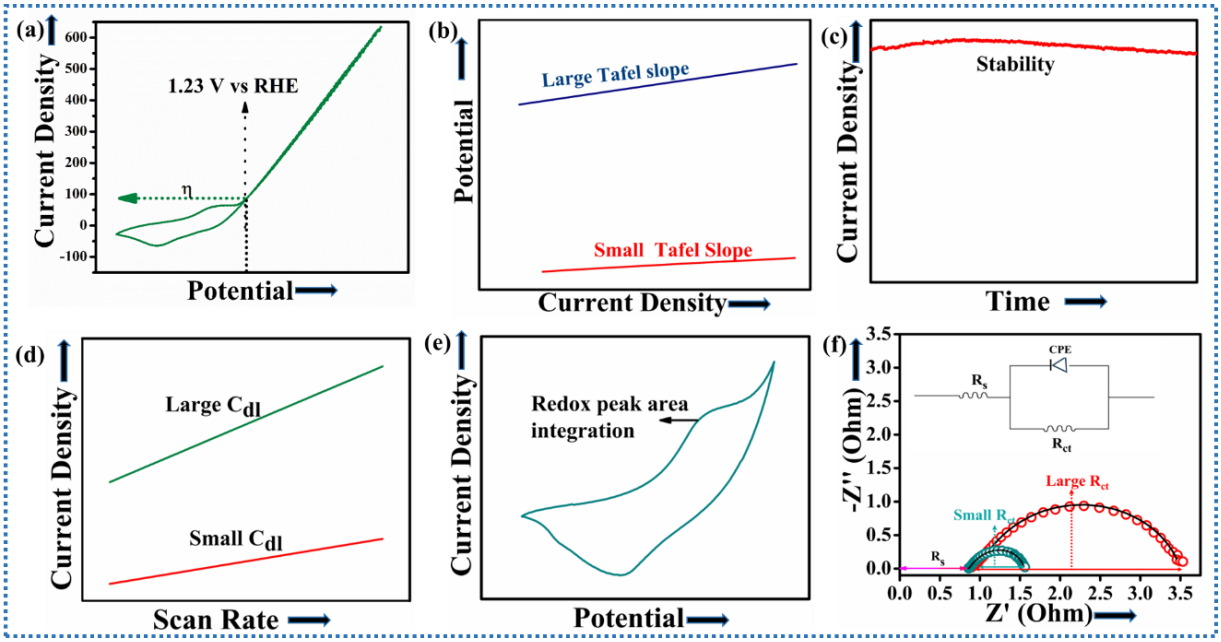

Figure 1.3. (a) Cyclic voltammetry curve illustrating OER; (b) Tafel plots displaying electrocatalyst performance for OER; (c) Cyclic voltammetry profile demonstrating redox peaks for determining surface active sites of an electrocatalyst, (d) (C_{dl}) plot for calculating the electrochemically active surface area (ECSA); (e) Stability test using chronoamperometry for an OER electrocatalyst; (f) Nyquish plot obtained from electrochemical impedance spectroscopy.

Impedance accounts not only for resistance but also for additional factors like inductance and capacitance. In electrochemical impedance spectroscopy (EIS), an alternating current (AC) voltage is applied to a sample across a range of frequencies, and the resulting electrical current is measured.[30] It can be utilized to study multiple electrochemical processes occurring simultaneously, determine the electron transfer rate of reactions, examine diffusion-controlled reactions, and characterize the system's capacitive behaviour. Impedance data aids in assessing the catalytic activity of a catalyst material and electrolyte by measuring the charge transfer resistance at the electrode/electrolyte interface and by measuring the rate of ion diffusion within the catalyst layer.[31]

EIS is typically monitored between 0.01 Hz and 100 kHz using a constant potential as the applied potential, which is the frequency range at which the investigated electrocatalyst can show detectable activity.[32] The resulting EIS plot is fitted with an equivalent circuit which can be divided into zones at low, moderate, and high frequencies, respectively which consists of electrolyte resistance (R_s), charge transfer resistance (R_{ct}) and a constant phase element . In an EIS plot, the electrolyte resistance (R_s) is determined from the intersection point of the high-frequency region and the horizontal axis and the charge transfer resistance (R_{ct}) is determined from the diameter of the semicircles in the low-frequency region (Figure. 1.3 f). A smaller R_{ct} indicates better charge transfer capability and stronger electronic conductivity, both of which lead to a faster reaction rate.[33] Thus, efficient catalysts are those which have lowest R_{ct} value.

1.3. Electrocatalysts for OER based on transition metal

Electrocatalysts based on transition metal have been the focus of much research to date owing to their outstanding OER catalytic activity.[34] However, the OER electrocatalysts based on transition metal can be classified into two main groups- the first one is based on precious metals and the

second one is based on earth-abundant transition metals.

Nobel metal-derived alloys, oxides, and composites as well as noble metals themselves exhibit significant OER activity in both alkaline and acidic conditions which makes them state-of-the-art -art electrocatalysts. Among these, Ru and Ir are known to perform better than Pt, Pd, and Rh.[35] Due to the high voltage employed during the OER process, noble-metal oxides like IrO_2 and RuO_2 have been chosen as the state-of-the-art catalysts for OER.[36][37] However, RuO_2 is extremely unstable in high anodic potential circumstances in both acidic and alkaline electrolytes. Although IrO_2 is more stable than RuO_2 and can persist at higher anodic potential, it still suffers from the same stability issues.[38] Therefore, their industrial-level application at a large scale is greatly hindered by their exorbitant price, inadequacy, and relatively insufficient stability.[39]Consequently, significant attempts have been dedicated to study the high performance of electrocatalysts that do not solely rely on noble metals In addition to noble metal electrocatalysts, non-noble metal electrocatalysts constitute a substantial portion of transition metal electrocatalysts and have been extensively reported to demonstrate exceptional catalytic activity, sometimes even outperforming noble metal electrocatalysts. [40] Consequently, significant attempts have been dedicated to study the high performance of electrocatalysts that do not solely rely on noble metals. Non-noble metal-based electrocatalysts, generally based on Co, Ni, Fe, and Mn, have been extensively studied in the past decade for their affordability, environmentally friendly nature, and easy conversion to the active phase during OER as well.[41] [42]

A number of techniques such as modulation of compositions, doping heteroatoms, morphological control, introducing defects in structure, and the formation of the hetero-structural interface, have been investigated to enhance the quantity of active site and speed up the catalytic process.[43] The OER performances of some noble-metal-free electrocatalysts have been found to

be equivalent or superior to those of electrocatalysts based on noble metals.[44] Recently, the developments in transition metal-based electrocatalysts for the OER can be categorized into hydroxides, oxyhydroxides, chalcogenides, nitrides, phosphides, and alloys.[45]

In our thesis, we have discussed the synthetic strategy and catalytic performance of transition metal-based layered double hydroxides (LDHs). The distinctive structural properties of LDHs, such as their tuneable composition, exchangeable intercalated anions, and single-atomic dispersion of high valence metallic cations (two or more species can be single atomically dispersed), have made them a novel class of inexpensive electrocatalysts for the OER in alkaline media.[46][47]

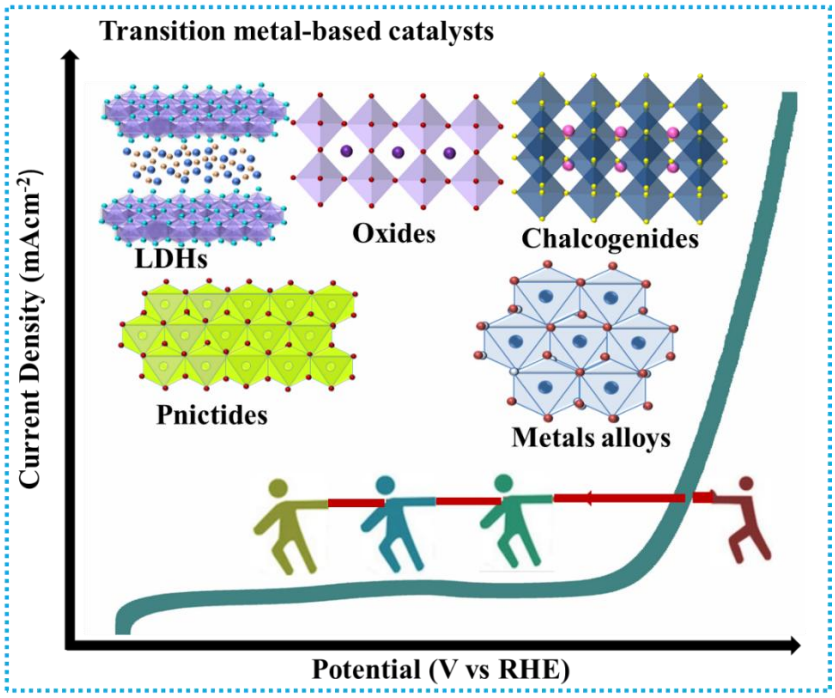

Figure 1.4. Image showing the possible approaches for improving performance for OER using transition metal-based electrocatalysts.

1.4. Layered double hydroxides (LDHs)

Out of the prevalent TM-based OER catalysts, layered double hydroxide (LDHs) nanosheets, have risen as highly proficient catalysts for OER owing to their distinctive layered structures and

electrocatalytic activity.[48] LDHs possess a comparable chemical composition represented as $[M^{II}_{1-x}M^{III}_{x}(OH)_2]^{x+}(A^{n-})_{x/n}$ .mH_2O, comprising a brucite-like layer of $M^{II}(OH)_2$ where some M^{II} cations are isomorphically replaced by M^{III} cations. Divalent (Ni^{2+}, Co^{2+}, Cu^{2+}, Zn^{2+}) and trivalent (Fe^{3+}, Mn^{3+}, Al^{3+}) metal cations are enabled to assemble into electropositive laminates through covalent interaction while anions exist between these two layers.[49][50] These anions are connected to the metallic element-containing layers by weak interactions like electrostatic interaction and hydrogen-bond interaction. These two-dimensional materials have drawn enormous interest for the OER owing to their high ratio of surface and bulk and significantly enhanced exposure of catalytic active sites than 0D and 1D materials. [51]

Typically, the methods used for the synthesis of LDHs are classified into two categories: the Top-down approach and the Bottom-up approach.[52] The top-down method is a two-step process and follows the swelling mechanism. This includes the exfoliation of pre-synthesized bulk LDHs with appropriate solvents.[53] Bottom-up synthesis method also known as the direct synthesis method is the simplest approach for the synthesis of LDHs as it does not need pre-synthesized LDHs. Structure of LDHs can be regulated by using appropriate temperature and solvents. [54][55]

Moreover, the ability to modify layered structures in a controllable manner (such as intercalation, topological adjustments, and integration of various materials) can result into excellent OER electrocatalyst.[56] The flexibility to modify chemical composition with differing cation ratios, the presence of hierarchical porosity facilitates the water molecule diffusion and gaseous product release.[57]

The strong electrostatic forces between layers and interlayer anions leads to organized arrangement of interlayer elements, and the potential for tailored arrangement of reactive sites. [58]All these aforementioned factors collectively contribute to increased structural durability and performance

enhancements of LDHs.[59][60] Thus, the OER activity of LDHs can be improved by i) electronic modulation which is achieved through a) cationic regulation b) anionic regulation c) defect engineering d) Interplanar distance modulation ii) self-supported approaches iii) heterojunction formation iv) the formation of ultrathin nanosheets.[61][62][63]

The cationic/anionic regulation was shown to be an efficient way to modulate the OER activity. In this process, vacancies can be created either by replacing the cations/anions or by etching method.[12][64] Cationic/anionic regulation can lead to the tuning of coordination environment and formation of defects of catalysts which results into exposure of more active sites and improved electrical conductivity.[65][66] Moreover, doping atoms can potentially operate as active sites to boost LDH catalysts' intrinsic activity.[67]

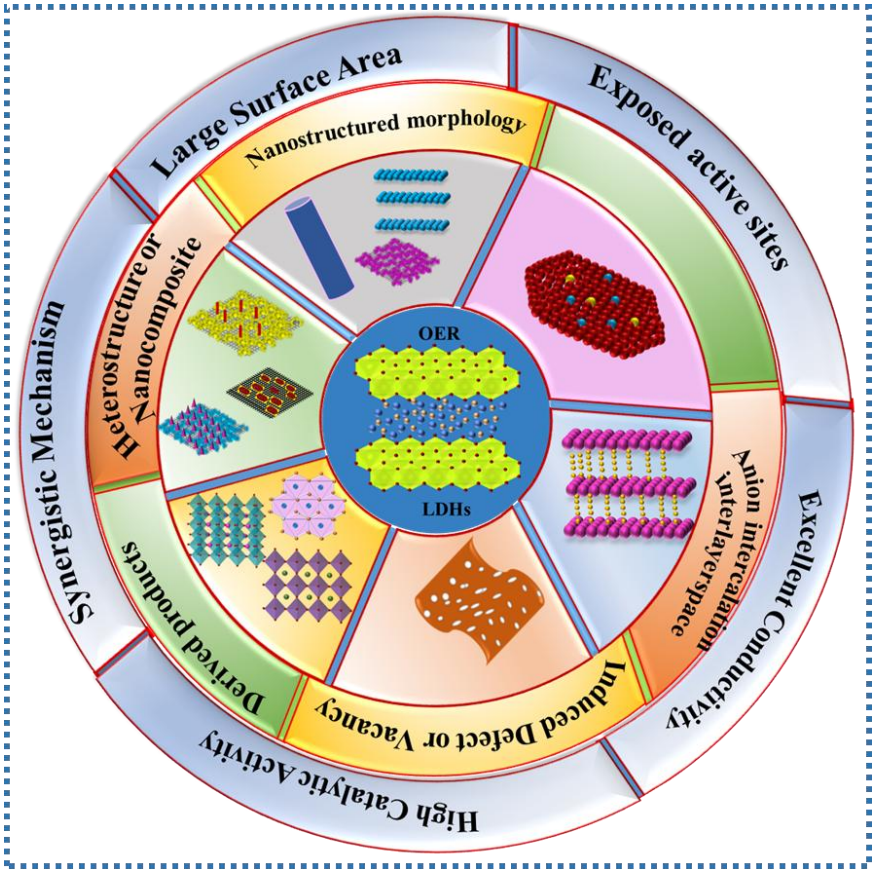

Figure 1.5. Strategies for modulation of LDH-based electrocatalysts for HER and OER.

Cationic regulation can be achieved by doping, etching, forming metal vacancies, or using different cations.[68] In 2018, Li et al. achieved efficient OER catalyst just by introducing cationic vacancies. They synthesized vanadium-doped NiFe-LDH which exhibited superior OER activity with reduced overpotential and Tafel slope in comparison to NiFe-LDH.[69] Yan et al. developed W^{6+} doped $Ni(OH)_2$ nanosheet sample to optimize the adsorption energy of the intermediate, thus leading to an obvious improvement in the OER activity because the low d^0 W^{6+} possesses more outermost empty orbitals which facilitates more adsorption of water and OH^- groups on the exposed W sites of the $Ni(OH)_2$ nanosheet.[70] It has been observed by several research group that anionic species can be successfully regulated to change their electrical properties and generate more reactive sites. This method allows for the modulation of LDH ionic-covalencies, which enhances ion transport between LDH layers and leads to very high reaction kinetics.

Introducing defects in the structure can regulate the electronic structure surrounding the active site near the defect site.[71] Specifically, it changed the distribution of electronic charge and increased the degree of disorder and exposed more active sites. Furthermore, defects in the catalyst can generate more surface metal atoms with low coordination numbers and additional dangling bonds, resulting in increased surface energy and a greater number of electrocatalytic sites.[72] Introduction of metal cationic vacancies in LDHs which can modulate the surface electronic structure surrounding the reactive sites and greatly increase electrocatalytic activity as the cationic vacancies in the catalyst can adjust the valence state of nearby metal centres, and thus leads to an excellent OER activity.[73][74] For example, Wang's group developed two NiFe LDHs nanosheets, with Ni^{2+} or Fe^{3+} vacancies (represented as NiFe LDHs-V_{Ni} and NiFe LDHs-V_{Fe}). NiFe-LDHs-V_{Fe} and NiFe-LDHs-V_{Ni} nanosheets demonstrated good OER catalytic activities with lower overpotentials equal to 245 and 229 mV at the current density 10 mA cm^{-2} respectively as

compared to NiFe-LDH, which can be attributed to optimized surface electronic structure of the active sites around Fe, or the Ni vacancies and the unsaturated coordinated sites generated by the introduction of the Fe or Ni vacancies.[75][76]

The most prevalent type of anionic vacancy are oxygen vacancies. Proper oxygen vacancies can change the electronic structure of the catalyst, increase the active sites, improve electrical conductivity, and optimize the adsorption energies of the OER intermediates.[77][78][79] For instance, Xiong's group developed NiFe-LDH with oxygen defects by treating with $NaBH_4$. The as synthesized NiFe-LDH with oxygen vacancy demonstrated exceptional OER activity with low overpotential of 200 mV for 10 mA cm^{-2} of current density.[80]

Inter planar distance modulation has been identified as an efficient approach for the enhanced OER activity of LDH.[81] It has been observed that increasing interlayer distance results in enhance OER activity because increasing interlayer distance can expose more active sites, boost mass and charge transfer efficiency. Interplanar distance modulation can be achieved through intercalation of various anions. Interplanar distance modulation can be achieved through intercalation of various anions.[82] For instance, Zhong et al. varied the interspace distance between 7.6 and 24.9 Å by inserting sodium dodecyl sulfate (SDS) into the layer space of NiFe-LDH nanosheets NiFe-LDH nanosheets' overpotential dropped from 333 mV to 289 mV as interspaces increased, which helped the OER process. [83]

Bulk LDHs suffer from insufficient electro-active sites therefore they are rarely used for EWS whereas ultrathin LDHs have more exposed active sites as compared to bulk LDHs.[84] Therefore, to overcome this problem, converting bulk LDHs into ultrathin LDHs has emerged as effective way to promote the OER activity of LDHs.[85] Hou et al. prepared ultrathin NiFeLDH through a facile and fast co-precipitation method at room temperature. As synthesized ultrathin NiFe-LDH

nanosheets demonstrated superior OER activity as it required low overpotential of 263 mV to achieve 10 mA cm^{-2} current density with long lasting durability in strong alkaline solution.[86]

In this sequence, another key strategy for increasing electrocatalytic activity is the fabrication of heterostructure catalysts.[87] The formation of a heterostructure might result in an internal electric field within the catalyst arising from arising from variations in the band structures of its two constituents.[88] [89] It enhances the catalytic activity by promoting the redistribution and transfer of charges via the integrated electric field at the interface.[90][91] Zhang et. al developed 3D hierarchical heterostructure NiFe-LDH@NiCoP/NF with enhanced bifunctional activity. HR-TEM characterization of the catalyst confirmed the formation of heterojunction between NiFe - LDH and NiCoP.[92] Liu et al. synthesized NiFe@NiCr-LDH heterostructure through a facile two-step hydrothermal technique as highly efficient OER catalyst. It required only 266 mV of overpotential to access the current density of 10 mA cm^{-2}.[93]

Additionally, another key strategy for increasing catalyst activity is the self-supported method, which involves direct growth of catalysts on conductive supports (such as graphene, carbon cloth, copper foam, nickel foam, etc.) without the use of non-conductive binder polymers.[94] Self-supported electrocatalysts demonstrate superior effectiveness and competitiveness in electrochemical water splitting compared to free-standing powders, owing to several advantages. This approach enhances long-term durability and electrocatalytic activity at high current densities, facilitating efficient charge and ion transfer through improved electrolyte-electrocatalyst contact.[95][96]

Despite the significant strides in research aimed at establishing transition metal based LDH as an effective OER catalyst, the understanding of the core elements responsible for its remarkable water oxidation performance is still constrained because of low conductivity, limited capacity to

transport electrons and charges as well as a lack of active edge sites, particularly for LDHs in their bulk form. For instance, how the synergistic interaction between the divalent and trivalent cations influence OER is still unknown.

Therefore, we have aimed to provide an overview of recent progress in TM LDHs involving unary, binary, and ternary transition-metal ions, focusing specifically on the influence of metal combinations that exert significant effects on OER activity.

1.5. Metal-organic framework-derived LDHs for OER

Metal-organic frameworks (MOFs) are formed by combining metal ions and organic ligands which are responsible for embodying qualities inherent to both homogeneous and heterogeneous catalysts.[97] MOFs and their derived materials have been extensively employed as OER electrocatalysts owing to their several benefits like large surface area, abundant pore structures, various compositions, and precisely defined metal centres.[98][99] More specifically, the substantial surface area boosts the accessibility of numerous active sites, the porous structure enables expeditious mass transportation, and the precisely defined metal centres play a vital role in mechanistic investigations.[100] Thus, in comparison to MOF, MOF-derived materials not only possess the advantages of MOF but also bear good conductivity and strong durability during water splitting.[101][102]

The primary challenge regarding MOF catalysis, especially in water and other strongly polar solvents, is their limited stability. This greatly diminishes their applicability in OER electrocatalysis.[103] In this regard, the use of MOF-Derived LDHs is emerging as a promising technology with substantial potential in the area of electrocatalysis and energy storage applications. MOF can be used to generate the ultrathin LDHs which significantly improves the OER activity.[104][105] LDH Derived from MOFs exhibit low crystallinity due to their abundant

pores on the surface. This leads to the display of a largely exposed surface area, tuneable metallic active sites, and good integrated conductivity, which makes them highly suitable for electrochemical applications.[106]

In this reference, Dong et al. constructed Ni-BDC@NiFe-LDH having ultrathin nanosheets structure using Ni-BDC as precursor. This catalyst exhibited demonstrated excellent electrocatalytic activity during OER as it required low overpotential of 264 mV to produce current density of 10 mA cm^{-2} and a lowest Tafel slope of 45 mV dec^{-1} in 1.0 M KOH.[107]

Xu et al. developed Ni-Fe-Ce-LDH microcapsule by one step synthetic approach using MIL-88 A as precursor. Superior OER performance was established by the special 3D Ni-Fe-Ce-LDH microcapsules, which produced 10 mA cm^{-2} current density using only low overpotential of 242 mV with long-term durability for at least 24 hours.[108]

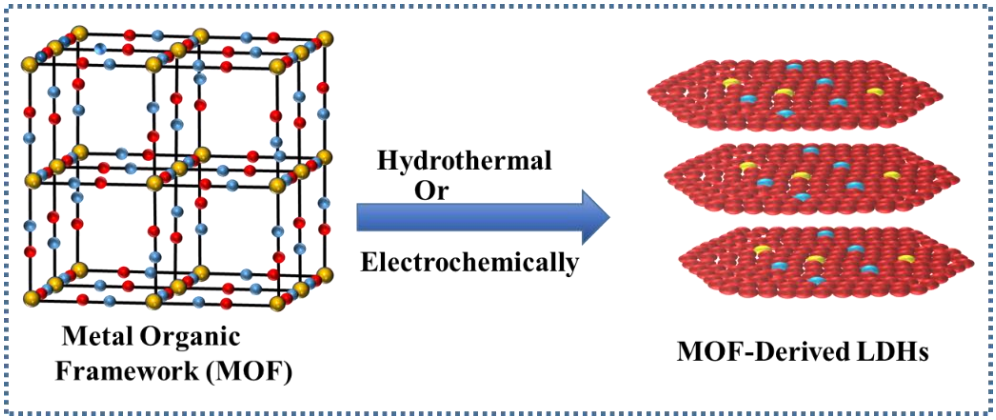

Figure 1.6. Schematic representation for the synthesis of LDHs from different types of MOFs.

1.6. Zeolitic imidazolate frameworks (ZIFs)

As a prominent subclass of MOF, Zeolitic imidazolate frameworks (ZIFs) have gained more attention for electrochemical energy conversion.[109] ZIFs comprise metal-imidazolate-metal moieties (like Co, Ni, Zn, etc.) in which tetrahedral metal centres, are coordinated by the nitrogen

atoms in the imidazole ligand's 1,3-positions. (Scheme 1).[110][111] This subclass of MOF is named ZIF due to the structural resemblance between MOF and inorganic aluminosilicate zeolites, in which metal ions represent the aluminium or silicon, and the organic linker, 2-methyl imidazole mimics the oxygen.[112] ZIFs exhibit characteristics that blend the properties of both MOFs and zeolites, offering a combination of advantages from both structures. These include high crystallinity, ultrahigh surface area, uniform micropores, tailored functionalities, and outstanding thermal and chemical stability.[113] Even within zinc and cobalt-based zeolitic imidazolate frameworks, the metal-imidazolate-metal angle closely resembles 145°, similar to the Si-O-Si angle observed in several zeolites **(Figure 1.7).**[114][115]

Therefore, zeolitic imidazolate frameworks (ZIFs) are highly regarded as exceptional precursors for producing catalytic materials known for their high activity and resilience against poisoning and corrosion.[116] Amongst the range of Zeolitic Imidazolate Frameworks (ZIFs), ZIF-67 stands out as a self-assembled structure in which Co^{2+} featuring an interconnection of cobalt (Co^{2+}) metal ions with the organic compound 2-methylimidazole (HmiM).[117]

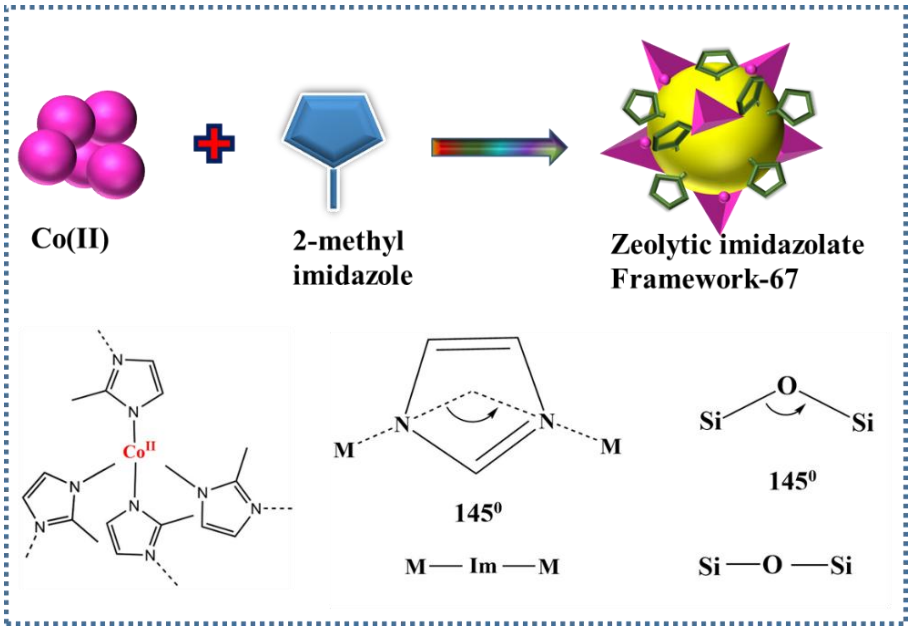

Figure 1.7. Illustration of structure of ZIF and similarity with zeolite.

1.6.1. ZIFs as OER electrocatalysts

ZIFs can be directly used for electrochemical processes owing to the presence of cobalt as redox-active metal, 2-methylimidazole as organic functionalities, well-structured coordination spheres, and adjustable pore sizes.[118][119] For example, Xu et al. employed pure ZIF-67 as electrocatalysts for the oxygen evolution reaction.[120] A decrease in overpotential was seen in the pH-dependent analytical investigation as the pH value increased. Additionally, ZIF-67 demonstrated stability beyond 3000 cycles in both basic and acidic solutions during the cycling stability test. However, the low conductivity and poor chemical stabilities of ZIFs in the reaction medium constrain its direct use in electrochemical processes.[121][122]

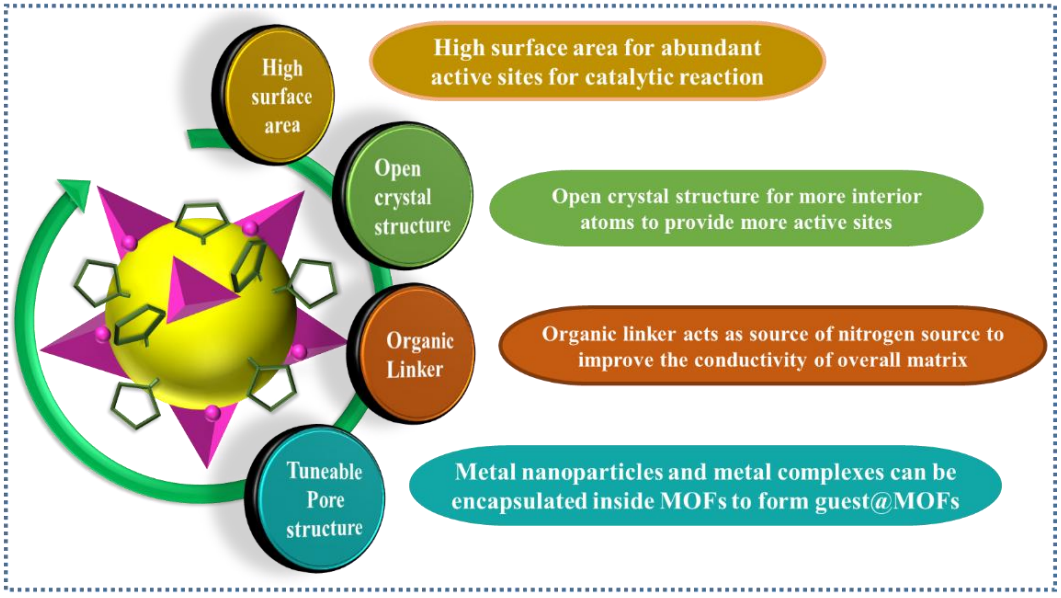

Figure 1.8. The advantages of the ZIF-67 as OER catalysts.

ZIF-67 demonstrates remarkable intrinsic activity in water oxidation which can be to the appropriate binding energy of OER intermediates containing cobalt. Owing to its structural instability, ZIF-67 can serve as a sacrificial template to form oxides, phosphides, hydroxides, and

other compounds featuring well-preserved porous architectures.[123]

In this thesis, we have demonstrated highly active OER catalysts derived from ZIF-67.

1.6.2. ZIF-67 Derived LDHs for OER

According to recent studies, zeolitic imidazolate frameworks (ZIFs), have flexible compositions and tuneable porosity structures, which make them ideal templates and versatile precursors for the synthesis of a variety of nanomaterials. However, the inherent low conductivity and the tendency of ZIF-67 derivatives to self-aggregate frequently give rise to increased overpotentials, leading to suppression in exposure of ZIF-67 surface active sites and a retardation in interfacial reaction kinetics.[124] Consequently, there exists an insufficiency of reports regarding the direct utilization of ZIFs in electrochemical water splitting. Also, it suffers from low stability in the reaction intermediate. Therefore, it is highly desirable to transform the ZIF-67 into a functional material. ZIF-67-derived LDHs are one of the most OER-active materials which possesses improved conductivity, greater stability, more exposed facets, and large surface area.

In 2017, Wang et al. successfully developed NiCo-LDH nanocages by a facile and simple technique using ZIF-67 as a sacrificial template and Co source. They employed it as OER catalysts in alkaline media and exhibited excellent OER catalytic activity as well as long-term stability.[125] Hue et al. synthesized FeCo-LDH@NF from ZIF-67 via hydrolysis reaction which exhibited remarkable OER activity as it required low overpotentials of 216.8 and 291.3 mV at j =10 and 100 mA cm^{-2}, respectively.[126] In this row, Lin et al. developed NiFeCo-LDH/CF from ZIF-67 by solvothermal process demonstrated superior OER activity with an overpotential of 249 mV at 10 mA cm^{-2} as well as long term durability for 20 h.[127]

Despite the fact that LDHs-derived materials have proven to be auspicious OER electrocatalysts because of their numerous advantages, such as affordability, widespread availability, and favorable

water adsorption properties, their electrocatalytic performance and practical application are severely hampered by the low intrinsic conductivity and poor durability of the powdery LDHs. More crucially, a nonconductive polymer binder is required to adhere the powdery LDH catalyst to conductive support for electrode fabrication. On the other hand, the use of a non-conductive binder greatly elevates the charge-transfer resistance of the electrode. Conversely, the generation of robust bubbles during the OER process may weaken the bond between the powdered LDHs and the substrate, ultimately causing the catalyst to spell out from the electrode surface.

In our thesis work, we have focused on self-supported LDHs which have been derived from self-supported ZIF-67.

1.7. Motivation and objective of thesis

The primary goal of this thesis is to establish a straightforward technique for the synthesis of self-supported M-Co-LDH catalysts by employing ZIF-67 as the precursor and the primary source of Co. In this context, research has been conducted on catalyst design, comprehension of the electronic structure of the active catalyst, and the utilization of these catalysts in oxygen evolution reactions. We have employed self-supported ZIF-67 to synthesize heterometal doped M-Co-LDH to achieve better OER performance. We also optimized the amount of heterometal to achieve the required OER performance. The specific objectives of this thesis have been divided into six chapters which are listed below.

In chapter-1 we have discussed electrochemical water oxidation (WOR), its basic evaluation parameters, and its importance in the area of energy conversion. We have also discussed the catalysts used for OER which include a brief description of electrocatalysts derived from noble metal, transition metal, LDHs, MOF-derived LDHs, and ZIF-Derived LDHs.

In chapter-2, we used the strategy of doping of high valent heterometal in the structure Co-

LDH derived from ZIF-67**.** For this purpose**,** we have demonstrated the easy synthetic approach for the synthesis of hierarchical hollow V_xCo-LDH layered double hydroxide (LDH) nanocages using ZIF-67. We have investigated the effect of change in the amount of V on the activity of V_xCo-LDH, revealing that all V_xCo-LDHs demonstrated better OER activity than Co-LDH. Excellent OER activity was achieved in alkaline medium by using the as-synthesized catalyst. Thus, inclusion of high valent vanadium is seen to boost water oxidation activity by modulating the electronic structure of Co^{2+} and assisting the Co centers-in reaching a high oxidation state (IV).

In chapter-3, In this chapter, we have employed self-supported LDH having atomic level thickness to get improved OER performance. To achieve this goal, we have demonstrated the hydroxylation of ZIF-67supported on nickel foam, assisted by Lewis acid Fe(III) via simple hydrothermal technique, resulting in the formation of ultrathin Fe_xCo-layered double hydroxide (LDH) nanosheets. The catalyst $Fe_{0.4}Co$-LDH exhibited exceptional water oxidation activity, achieving a current density of 20 mA cm² at a mere 190 mV overpotential. This performance is superior to that of hydrothermally synthesized LDH with a similar composition.

Further, **in chapter-4** We demonstrated the electrochemical reconstruction of ZIF-67 during anodic water oxidation, resulting in the formation of FeCo-LDH-x [Fe-$Co(OH)_2$/Co(O)OH] (where x = 1, 2, 3, 4, 5). Fe(III) ions present in the electrolyte solution are incorporated into the structure of the active catalyst during the anodic reconstruction of ZIF-67. The electrochemically derived FeCo-LDH-x exhibits a high electrochemical surface area, numerous exposed active sites, atomic-level thickness, and optimized structural and electronic features, leading to improved OER activity. The activity of all FeCo-LDH-x catalysts was found to be superior to that of the as-synthesized Co-LDH-3. Out of all synthesized catalysts, FeCo-LDH-3 showed the best OER performance, achieving a current density of 50 mA cm^{-2} at an overpotential of 180 mV, along with

the lowest Tafel slope value and charge transfer resistance.

In chapter-5, we used a hydrothermal approach to introduce the f-block element Ce to ZIF-67@NF. This led to the development of the CeO_2/CeCoLDH heterostructure, where the water oxidation reaction is aided by the overlap of the 4f-2p-3d orbitals. 4f-2p-3d orbital overlap modulated the electronic structure and obtained heterostructure regulated the transportation of charges during the OER process. 4f-2p-3d orbital overlap demonstrated the more proficient delocalization of π-electron density over metal cavity via oxide bridging in comparison to 3d-2p-3d overlap. Thus, the as-obtained CeO_2/Ce-Co-LDH heterostructures exhibited excellent OER performance and stability.

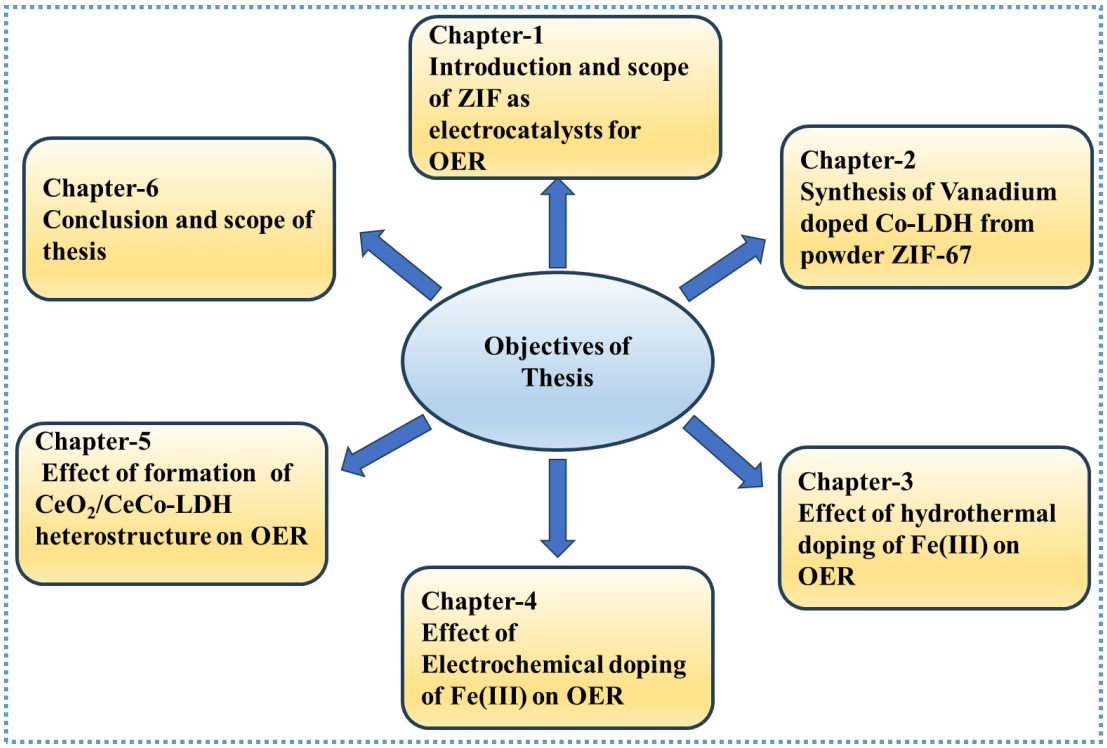

Figure 1.9. Chapter-wise objectives of the thesis.

Chapter-6 presents a concise review of the scientific contributions made in this thesis, highlighting the outcomes of our research, which offer essential insights for developing efficient

and cost-effective electrocatalysts derived from self-supported ZIF-67 for improved electrochemical energy conversion process. Additionally, we have discussed the future perspectives of ZIF-67-derived electrocatalysts.

1.8. References:

[1] Z. Zand, P. Salimi, M. R. Mohammadi, R. Bagheri, P. Chernev, Z. Song, H. Dau, M. Görlin, M. M. Najafpour, *ACS Sustain. Chem. Eng.* **2019**, *7*, 17252.

[2] Y. Zhao, N. Dongfang, C. A. Triana, C. Huang, R. Erni, W. Wan, J. Li, D. Stoian, L. Pan, P. Zhang, J. Lan, M. Iannuzzi, G. R. Patzke, *Energy Environ. Sci.* **2022**, *15*, 727.

[3] D. Chen, R. Lu, R. Yu, Y. Dai, H. Zhao, D. Wu, P. Wang, J. Zhu, Z. Pu, L. Chen, J. Yu, S. Mu, *Angew. Chemie - Int. Ed.* **2022**, *61*, 2208642.

[4] P. Chen, T. Zhou, S. Wang, N. Zhang, Y. Tong, H. Ju, W. Chu, C. Wu, Y. Xie, *Angew. Chemie - Int. Ed.* **2018**, *57*, 15471.

[5] H. Yang, M. Driess, P. W. Menezes, *Adv. Energy Mater.* **2021**, *11*, 2102074.

[6] S. Anantharaj, S. Noda, V. R. Jothi, S. C. Yi, M. Driess, P. W. Menezes, *Angew. Chemie - Int. Ed.* **2021**, *60*, 18981.

[7] Z. Zou, T. Wang, X. Zhao, W. J. Jiang, H. Pan, D. Gao, C. Xu, *ACS Catal.* **2019**, *9*, 7356.

[8] L. Chen, J. T. Ren, Z. Y. Yuan, *Green Chem.* **2022**, *24*, 713.

[9] K. Zhang, R. Zou, *Small* **2021**, *17*, 2100129.

[10] H. Sun, X. Xu, H. Kim, W. C. Jung, W. Zhou, Z. Shao, *Energy Environ. Mater.* **2023**, *6*, e12441.

[11] B. H. R. Suryanto, Y. Wang, R. K. Hocking, W. Adamson, C. Zhao, *Nat. Commun.* **2019**, *10*, 13415.

[12] D. Wang, Q. Li, C. Han, Q. Lu, Z. Xing, X. Yang, *Nat. Commun.* **2019**, *10*, 3899.

[13] T. Guo, L. Li, Z. Wang, *Adv. Energy Mater.* **2022**, *12*, 2200827.

[14] H. N. Nong, L. J. Falling, A. Bergmann, M. Klingenhof, H. P. Tran, C. Spöri, R. Mom, J. Timoshenko, G. Zichittella, A. Knop-Gericke, S. Piccinin, J. Pérez-Ramírez, B. R. Cuenya, R. Schlögl, P. Strasser, D. Teschner, T. E. Jones, *Nature* **2020**, *587*, 408.

[15] J. Liang, X. Gao, B. Guo, Y. Ding, J. Yan, Z. Guo, E. C. M. Tse, J. Liu, *Angew. Chemie - Int. Ed.* **2021**, *60*, 12770.

[16] X. Lei, Q. Tang, Y. Zheng, P. Kidkhunthod, X. Zhou, B. Ji, Y. Tang, *Nat. Sustain.* **2023**, *6*, 816.

[17] P. W. Menezes, S. Yao, R. Beltrán-Suito, J. N. Hausmann, P. V. Menezes, M. Driess, *Angew. Chemie* **2021**, *133*, 4690.

[18] S. Wang, Q. Jiang, S. Ju, C. S. Hsu, H. M. Chen, D. Zhang, F. Song, *Nat. Commun.* **2022**, *13*, 34380.

[19] S. Anantharaj, S. Kundu, *ACS Energy Lett.* **2019**, *4*, 1260.

[20] H. Dau, C. Limberg, T. Reier, M. Risch, S. Roggan, P. Strasser, *ChemCatChem* **2010**, *2*, 724.

[21] B. Singh, A. Yadav, A. Indra, *J. Mater. Chem. A* **2022**, *10*, 3843.

[22] A. Raveendran, M. Chandran, R. Dhanusuraman, *RSC Adv.* **2023**, *13*, 3843.

[23] S. Anantharaj, S. R. Ede, K. Sakthikumar, K. Karthick, S. Mishra, S. Kundu, *ACS Catal.* **2016**, *6*, 8069.

[24] H. Vrubel, T. Moehl, M. Grätzel, X. Hu, *Chem. Commun.* **2013**, *49*, 8985.

[25] S. Anantharaj, P. E. Karthik, S. Noda, *Angew. Chemie - Int. Ed.* **2021**, *60*, 23051.

[26] S. Sun, H. Li, Z. J. Xu, *Joule* **2018**, *2*, 1024.

[27] S. Anantharaj, S. R. Ede, K. Karthick, S. Sam Sankar, K. Sangeetha, P. E. Karthik, S.

Kundu, *Energy Environ. Sci.* **2018**, *11*, 744.

[28] S. Wang, J. Zhang, O. Gharbi, V. Vivier, M. Gao, M. E. Orazem, *Nat. Rev. Methods Prim.* **2021**, *1*, 46.

[29] A. C. Lazanas, M. I. Prodromidis, *ACS Meas. Sci. Au* **2023**, *3*, 162.

[30] R.G.V.K. Mohan, *J.App. Chem.* **2013**, *4*, 48.

[31] N. O. Laschuk, E. B. Easton, O. V. Zenkina, *RSC Adv.* **2021**, *11*, 27925.

[32] Z. Xu, Z. Wu, *eScience* **2024**, 100334, doi.org/10.1016/j.esci.2024.100334.

[33] Z. Y. Yu, Y. Duan, X. Y. Feng, X. Yu, M. R. Gao, S. H. Yu, *Adv. Mater.* **2021**, *33*, 2007100.

[34] M. Tahir, L. Pan, F. Idrees, X. Zhang, L. Wang, J. J. Zou, Z. L. Wang, *Nano Energy* **2017**, *37*, 136.

[35] Q. Shi, C. Zhu, D. Du, Y. Lin, *Chem. Soc. Rev.* **2019**, *48*, 3181.

[36] O. Kasian, J. P. Grote, S. Geiger, S. Cherevko, K. J. J. Mayrhofer, *Angew. Chemie - Int. Ed.* **2018**, *57*, 2488.

[37] X. Y. Wang, M. Zhu, Q. N. Bian, B. S. Guo, W. Q. Kong, C. Bin Wang, Y. Y. Feng, *ACS Appl. Nano Mater.* **2023**, *6*, 5200.

[38] R. Kötz, H. J. Lewerenz, P. Brüesch, S. Stucki, *J. Electroanal. Chem.* **1983**, *150*, 209.

[39] H. Zhang, Y. Liu, T. Chen, J. Zhang, J. Zhang, X. W. Lou, *Adv. Mater.* **2019**, *31*, 1900281.

[40] A. Indra, P. W. Menezes, C. Das, D. Schmeißer, M. Driess, *Chem. Commun.* **2017**, *53*, 8641.

[41] S. Anantharaj, V. Aravindan, *Adv. Energy Mater.* **2020**, *10*, 1902666.

[42] J. Melder, S. Mebs, F. Lessing, H. Dau, P. Kurz, *Sustain. Energy Fuels* **2022**, *7*, 92.

[43] X. Wang, L. Meng, B. Li, Y. Gong, *Mater. Today* **2021**, *47*, 108.

[44] D. Tan, H. Xiong, T. Zhang, X. Fan, J. Wang, F. Xu, *Front. Chem.* **2022**, *10*, 3389.

[45] S. Yang, X. Liu, S. Li, W. Yuan, L. Yang, T. Wang, H. Zheng, R. Cao, W. Zhang, *Chem. Soc. Rev.* **2024**, 5593.

[46] D. Zhou, P. Li, X. Lin, A. McKinley, Y. Kuang, W. Liu, W. F. Lin, X. Sun, X. Duan, *Chem. Soc. Rev.* **2021**, *50*, 8790.

[47] C. Han, Y. Zhao, Y. Yuan, Z. Guo, G. Chen, J. Yang, Q. Bao, L. Guo, C. Chen, *Int. J. Hydrogen Energy* **2024**, *63*, 918.

[48] P. Zhou, Y. Wang, C. Xie, C. Chen, H. Liu, R. Chen, J. Huo, S. Wang, *Chem. Commun.* **2017**, *53*, 11778.

[49] G. Fan, F. Li, D. G. Evans, X. Duan, *Chem. Soc. Rev.* **2014**, *43*, 7040.

[50] A. Hameed, M. Batool, Z. Liu, M. A. Nadeem, R. Jin, *ACS Energy Lett.* **2022**, *7*, 3311.

[51] L. Lv, Z. Yang, K. Chen, C. Wang, Y. Xiong, *Adv. Energy Mater.* **2019**, *9*, 1803358..

[52] X. Lu, H. Xue, H. Gong, M. Bai, D. Tang, R. Ma, T. Sasaki, *2D Layered Double Hydroxide Nanosheets and Their Derivatives Toward Efficient Oxygen Evolution Reaction*, Springer Singapore, **2020**.

[53] Y. Zhang, H. Xu, S. Lu, *RSC Adv.* **2021**, *11*, 24254.

[54] J. Yu, Q. Wang, D. O'Hare, L. Sun, *Chem. Soc. Rev.* **2017**, *46*, 5950.

[55] B. Singh, A. Indra, *Dalt. Trans.* **2021**, *50*, 2359.

[56] Y. Wang, D. Yan, S. El Hankari, Y. Zou, S. Wang, *Adv. Sci.* **2018**, *5*, 1800064.

[57] X. Zhao, P. Song, C. Wang, A. C. Riis-Jensen, W. Fu, Y. Deng, D. Wan, L. Kang, S. Ning, J. Dan, T. Venkatesan, Z. Liu, W. Zhou, K. S. Thygesen, X. Luo, S. J. Pennycook, K. P. Loh, *Nature* **2020**, *581*, 171.

[58] A. Karmakar, K. Karthick, S. S. Sankar, S. Kumaravel, R. Madhu, S. Kundu, *J. Mater. Chem. A* **2021**, *9*, 1314.

[59] G. Mishra, B. Dash, S. Pandey, *Appl. Clay Sci.* **2018**, *153*, 172.

[60] P. Roy Chowdhury, H. Medhi, K. G. Bhattacharyya, C. Mustansar Hussain, *Coord. Chem. Rev.* **2023**, *483*, 215083.

[61] L. Huang, Y. Zou, D. Chen, S. Wang, *Chinese J. Catal.* **2019**, *40*, 1822.

[62] Y. Zhu, X. Wang, X. Zhu, Z. Wu, D. Zhao, F. Wang, D. Sun, Y. Tang, H. Li, G. Fu, *Small* **2023**, *19*, 2206531.

[63] T. You, K. Deng, P. Liu, X. Lv, W. Tian, H. Li, J. Ji, *Chem. Eng. J.* **2023**, *470*, 144348.

[64] Z. Li, Y. Wang, L. Y. S. Lee, *Catalysts* **2023**, *13*, 1230.

[65] A. Mavrič, M. Valant, *Inorganics* **2023**, *11*, 296.

[66] J. Morales-Vidal, R. García-Muelas, M. A. Ortuño, *Catal. Sci. Technol.* **2021**, *11*, 1443.

[67] R. Li, D. Zhang, H. Chen, S. Wang, Y. Ling, C. Fang, *ACS Sustain. Chem. Eng.* **2023**, *11*, 16098.

[68] B. Singh, A. K. Patel, A. Indra, *Mater. Today Chem.* **2022**, *25*, 100930.

[69] K. Bera, A. Karmakar, S. Kumaravel, S. Sam Sankar, R. Madhu, H. N Dhandapani, S. Nagappan, S. Kundu, *Inorg. Chem.* **2022**, *61*, 4502.

[70] J. Yan, L. Kong, Y. Ji, J. White, Y. Li, J. Zhang, P. An, S. Liu, S. T. Lee, T. Ma, *Nat. Commun.* **2019**, *10*, 1 2149.

[71] J. Yu, Q. Cao, Y. Li, X. Long, S. Yang, J. K. Clark, M. Nakabayashi, N. Shibata, J. J. Delaunay, *ACS Catal.* **2019**, *9*, 1605.

[72] Z. Cai, Y. Bi, E. Hu, W. Liu, N. Dwarica, Y. Tian, X. Li, Y. Kuang, Y. Li, X. Q. Yang, H. Wang, X. Sun, *Adv. Energy Mater.* **2018**, *8*, 1701694.

[73] J. Zheng, X. Peng, Z. Xu, J. Gong, Z. Wang, *ACS Catal.* **2022**, *12*, 10245.

[74] H. Zhang, H. Guo, Y. Li, Q. Zhang, L. Zheng, L. Gu, R. Song, *Adv. Funct. Mater.* **2023**,

33, 2304403.

[75] Y. Wang, M. Qiao, Y. Li, S. Wang, *Small* **2018**, *14*, 1800136.

[76] M. Zubair, P. Kumar, M. Klingenhof, B. Subhash, J. A. Yuwono, S. Cheong, Y. Yao, L. Thomsen, P. Strasser, R. D. Tilley, N. M. Bedford, *ACS Catal.* **2023**, *13*, 4799.

[77] S. Ram, G. H. Choi, A. S. Lee, S. C. Lee, S. Bhattacharjee, *J. Phys. Chem. C* **2023**, *127*, 12576.

[78] H. Liang, H. Jia, T. Lin, Z. Wang, C. Li, S. Chen, J. Qi, J. Cao, W. Fei, J. Feng, *J. Colloid Interface Sci.* **2019**, *554*, 59.

[79] Y. H. Wang, L. Li, J. Shi, M. Y. Xie, J. Nie, G. F. Huang, B. Li, W. Hu, A. Pan, W. Q. Huang, *Adv. Sci.* **2023**, *10*, 2303321 .

[80] X. Xiong, Z. Cai, D. Zhou, G. Zhang, Q. Zhang, Y. Jia, X. Duan, Q. Xie, S. Lai, T. Xie, Y. Li, X. Sun, X. Duan, *Sci. China Mater.* **2018**, *61*, 939.

[81] Y. Zhao, T. Sun, Q. Yin, J. Zhang, S. Zhang, J. Luo, H. Yan, L. Zheng, J. Han, M. Wei, *J. Mater. Chem. A* **2019**, *7*, 15371.

[82] X. Li, X. Hao, Z. Wang, A. Abudula, G. Guan, *J. Power Sources* **2017**, *347*, 193.

[83] L. Li, Y. Dai, Q. Xu, B. Zhang, F. Zhang, Y. You, D. Ma, S. S. Li, Y. X. Zhang, *J. Alloys Compd.* **2021**, *882*, 160752.

[84] J. Duan, S. Chen, C. Zhao, *Nat. Commun.* **2017**, *8*, 15437.

[85] Y. Wang, Y. Zhang, Z. Liu, C. Xie, S. Feng, D. Liu, M. Shao, S. Wang, *Angew. Chemie - Int. Ed.* **2017**, *56*, 5867.

[86] C. Hou, Z. Cui, S. Zhang, W. Yang, H. Gao, X. Luo, *RSC Adv.* **2021**, *11*, 37624.

[87] X. Ding, R. Jiang, J. Wu, M. Xing, Z. Qiao, X. Zeng, S. Wang, D. Cao, *Adv. Funct. Mater.* **2023**, *33*, 2306786.

[88] J. Zhu, S. Mu, *Inorg. Chem. Front.* **2023**, *10*, 2220.

[89] J. Zhu, Q. Zeng, C. Yan, W. He, *ACS Appl. Nano Mater.* **2019**, *2*, 5604.

[90] F. Lin, Z. Dong, Y. Yao, L. Yang, F. Fang, L. Jiao, *Adv. Energy Mater.* **2020**, *10*, 2002176.

[91] Y. Zhang, L. You, Q. Liu, Y. Li, T. Li, Z. Xue, G. Li, *ACS Appl. Mater. Interfaces* **2021**, *13*, 2765.

[92] H. Zhang, X. Li, A. Hähnel, V. Naumann, C. Lin, S. Azimi, S. L. Schweizer, A. W. Maijenburg, R. B. Wehrspohn, *Adv. Funct. Mater.* **2018**, *28*, 1706847.

[93] S. Liu, Y. Tang, C. Guo, Y. Liu, Z. Tang, *Materials* **2023,** 16, 2968.

[94] H. Sun, Z. Yan, F. Liu, W. Xu, F. Cheng, J. Chen, *Adv. Mater.* **2020**, *32*, 1806326.

[95] P. Wang, B. Wang, *ACS Appl. Mater. Interfaces* **2021**, *13*, 59593.

[96] T. Y. Ma, S. Dai, S. Z. Qiao, *Mater. Today* **2016**, *19*, 265.

[97] L. Jiao, J. Y. R. Seow, W. S. Skinner, Z. U. Wang, H. L. Jiang, *Mater. Today* **2019**, *27*, 43.

[98] A. E. Baumann, D. A. Burns, B. Liu, V. S. Thoi, *Commun. Chem.* ***2019****, 2, 86.*

[99] Z. Xu, C.-L. Yeh, J.-L. Chen, J. T. Lin, K.-C. Ho, R. Y.-Y. Lin, *ACS Sustainable Chem. Eng.* **2022**, 10, 11586

[100] B. Singh, A. Singh, A. Yadav, A. Indra, *Coord. Chem. Rev.* **2021**, *447*, 214144.

[101] Q. N. Bian, B. S. Guo, D. X. Tan, D. Zhang, W. Q. Kong, C. Bin Wang, Y. Y. Feng, *ACS Appl. Mater. Interfaces* **2024**, *16*, 14742.

[102] M. Ding, J. Chen, M. Jiang, X. Zhang, G. Wang, *J. Mater. Chem. A* **2019**, *7*, 14163.

[103] W. Zheng, L. Y. S. Lee, *ACS Energy Lett.* **2021**, *6*, 2838.

[104] H. Zhang, X. Liu, Y. Wu, C. Guan, A. K. Cheetham, J. Wang, *Chem. Commun.* **2018**, *54*, 5268.

[105] H. F. Wang, L. Chen, H. Pang, S. Kaskel, Q. Xu, *Chem. Soc. Rev.* **2020**, *49*, 1414.

[106] Z. Song, J. Zhao, U. Ghani, W. Liu, B. Ye, X. Cai, *ChemElectroChem* **2024**, *11*, 2300731.

[107] Q. Dong, C. Shuai, Z. Mo, R. Guo, N. Liu, G. Liu, J. Wang, W. Liu, Y. Chen, J. Liu, Y. Jiang, Q. Gao, *CrystEngComm* **2021**, *23*, 1172.

[108] H. Xu, C. Shan, X. Wu, M. Sun, B. Huang, Y. Tang, C. H. Yan, *Energy Environ. Sci.* **2020**, *13*, 2949.

[109] L. Chen, Z. Huangfu, X. Yang, H. Lei, Z. Wang, W. Mai, *Inorg. Chem. Front.* **2024**, *20*, 2702.

[110] Q. Hong, Y. Wang, R. Wang, Z. Chen, H. Yang, K. Yu, Y. Liu, H. Huang, Z. Kang, P. W. Menezes, *Small* **2023**, *19*, 2206723.

[111] X. Guo, T. Xing, Y. Lou, J. Chen, *J. Solid State Chem.* **2016**, *235*, 107.

[112] Y. Zhang, L. Qi, *Nanoscale* **2022**, *14*, 12196.

[113] S. Dutta, Z. Liu, H. S. Han, A. Indra, T. Song, *ChemElectroChem* **2018**, *5*, 3571.

[114] K. S. Park, Z. Ni, A. P. Côté, J. Y. Choi, R. Huang, F. J. Uribe-Romo, H. K. Chae, M. O'Keeffe, O. M. Yaghi, *Proc. Natl. Acad. Sci. U. S. A.* **2006**, *103*, 10186.

[115] Z. Zheng, Z. Rong, H. L. Nguyen, O. M. Yaghi, *Inorg. Chem.* **2023**, *62*, 20861.

[116] L. Jiao, Y. X. Zhou, H. L. Jiang, *Chem. Sci.* **2016**, *7*, 1690.

[117] K. T. Butler, S. D. Worrall, C. D. Molloy, C. H. Hendon, M. P. Attfield, R. A. W. Dryfe, A. Walsh, *J. Mater. Chem. C* **2017**, *5*, 7726.

[118] K. Fujie, K. Otsubo, R. Ikeda, T. Yamada, H. Kitagawa, *Chem. Sci.* **2015**, *6*, 4306.

[119] P. Zhao, S. Fu, L. Cheng, Z. Jiao, M. Wu, *Coord. Chem. Rev.* **2024**, *498*, 215452.

[120] Q. Xu, H. Li, F. Yue, L. Chi, J. Wang, *New J. Chem.* **2016**, *40*, 3032.

[121] X. Cao, C. Tan, M. Sindoro, H. Zhang, *Chem. Soc. Rev.* **2017**, *46*, 2660.

[122] Z. Lei, X. Jin, J. Li, Y. Liu, J. Liu, S. Jiao, R. Cao, *J. Energy Chem.* **2022**, *65*, 505.

[123] Y. M. Jo, T. H. Kim, C. S. Lee, K. Lim, C. W. Na, F. Abdel-Hady, A. A. Wazzan, J. H. Lee, *ACS Appl. Mater. Interfaces* **2018**, *10*, 8860.

[124] J. Zhu, L. Hu, P. Zhao, L. Y. S. Lee, K. Y. Wong, *Chem. Rev.* **2020**, *120*, 851.

[125] C. Wang, J. Zhang, C. Shi, D. Cai, *Int. J. Electrochem. Sci.* **2017**, *12*, 10003.

[126] L. Hu, L. Tian, X. Ding, X. Wang, X. Wang, Y. Qin, W. Gu, L. Shi, C. Zhu, *Inorg. Chem. Front.* **2022**, *9*, 5296.

[127] Y. Lin, H. Wang, C. K. Peng, L. Bu, C. L. Chiang, K. Tian, Y. Zhao, J. Zhao, Y. G. Lin, J. M. Lee, L. Gao, *Small* **2020**, *16*, 2002426.